

Changes of the Molecular Mobility of Poly(ϵ -caprolactone) upon Drawing, Studied by Dielectric Relaxation Spectroscopy

Yang, Xiao Yan; Liu, Shao Shuai; Korobko, Alexander V.; Picken, Stephen J.; Besseling, Nicolaas A.M.

DOI

[10.1007/s10118-018-2030-1](https://doi.org/10.1007/s10118-018-2030-1)

Publication date

2018

Document Version

Final published version

Published in

Chinese Journal of Polymer Science (English Edition)

Citation (APA)

Yang, X. Y., Liu, S. S., Korobko, A. V., Picken, S. J., & Besseling, N. A. M. (2018). Changes of the Molecular Mobility of Poly(ϵ -caprolactone) upon Drawing, Studied by Dielectric Relaxation Spectroscopy. *Chinese Journal of Polymer Science (English Edition)*, 36(5), 665-674. <https://doi.org/10.1007/s10118-018-2030-1>

Important note

To cite this publication, please use the final published version (if applicable).
Please check the document version above.

Copyright

Other than for strictly personal use, it is not permitted to download, forward or distribute the text or part of it, without the consent of the author(s) and/or copyright holder(s), unless the work is under an open content license such as Creative Commons.

Takedown policy

Please contact us and provide details if you believe this document breaches copyrights.
We will remove access to the work immediately and investigate your claim.

Changes of the Molecular Mobility of Poly(ϵ -caprolactone) upon Drawing, Studied by Dielectric Relaxation Spectroscopy

Xiao-Yan Yang^{a*}, Shao-Shuai Liu^a, Alexander V. Korobko^b, Stephen J. Picken^b, and Nicolaas A.M. Besseling^b

^a Lucky Research Institute, China Lucky Group Corporation, Baoding 071054, China

^b Department of Chemical Engineering, Delft University of Technology, 2628 BL Delft, and Dutch Polymer Institute (DPI), 5600 AX Eindhoven, the Netherlands

Abstract Dielectric relaxation spectroscopy (DRS) of poly(ϵ -caprolactone) with different draw ratios showed that the mobility of polymer chains in the amorphous part decreases as the draw ratio increases. The activation energy of the α process, which corresponds to the dynamic glass transition, increases upon drawing. The enlarged gap between the activation energies of the α process and the β process results in a change of continuity at the crossover between the high temperature α process and the α and β processes. At low drawing ratios the α process connects with the β process, while at the highest drawing ratio in our measurements, the α process is continuous with the α process. This is consistent with X-ray diffraction results that indicate that upon drawing the polymer chains in the amorphous part align and densify upon drawing. As the draw ratio increases, the α relaxation broadens and decreases its intensity, indicating an increasing heterogeneity. We observed slope changes in the α traces, when the temperature decreases below that at which $\tau_{\alpha} \approx 1$ s. This may indicate the glass transition from the ‘rubbery’ state to the non-equilibrium glassy state.

Keywords Semicrystalline polymer; Dielectric relaxation spectroscopy; Molecular mobility

Citation: Yang, X. Y.; Liu, S. S.; Korobko, A. V.; Picken, S. J.; Besseling, N. A. M. Changes of the Molecular Mobility of Poly(ϵ -caprolactone) upon Drawing, Studied by Dielectric Relaxation Spectroscopy. Chinese J. Polym. Sci. 2018, 36(5), 665–674.

INTRODUCTION

An interesting question in materials science is how materials behave in a confinement. To answer this question, many studies^[1–3] have been done. Due to the fact that the polymer chains stretched in one dimension will behave the same as under confinement in other two dimensions, we select poly(ϵ -caprolactone) (PCL) as a model to study its dynamics in uniaxially drawn state. PCL is an increasingly important semicrystalline polymer. It is becoming a useful material in biomedical applications^[4–6]. As PCL is widely applied in fibers, the dynamics of uniaxially drawn PCL is of importance. When PCL samples are stretched in the solid state, necking occurs. In this article, the draw ratio λ is defined as the ratio of final length of drawn sample to the initial length of the undrawn sample. For PCL, the minimal draw ratio, which is when a drawn neck coexists with an undrawn region, is four. We will call this the ‘natural draw ratio’. Necking does not happen with every semicrystalline polymer^[7] but when necking occurs, the original spherulites convert to oriented fibrils upon drawing^[8–12]. A recrystallization under strain may occur with the help of pre-existing lamellae^[13–15]. A study on the morphology of

PCL upon uniaxial drawing in a PCL/poly(vinyl chloride) (PVC)^[16] blend shows that the crystalline chain orientation can be either parallel or perpendicular to the stretching direction, and that parallel chain orientation is dominant in the amorphous region.

The molecular dynamics of polymeric materials can be studied by dielectric relaxation spectroscopy (DRS). DRS probes the time scales and intensities of relaxation processes as a function of temperature. Similarly as that with dynamic rheology the frequency is varied, with DRS, an oscillatory electrical field is applied instead of an oscillating mechanical stress. In a DRS measurement one measures the so-called complex dielectric constant $\epsilon^* = \epsilon' + i\epsilon''$, where ϵ' represents the ‘storage’ contribution, and ϵ'' the ‘loss’ or ‘dissipation’ contribution. Dielectric relaxation processes can be associated with the motion of electrons around the atoms, of dipolar moieties and of ions. At very low temperature or very high frequency, only the electrons around the atoms of the material can follow the alternating electrical field. At higher temperature and/or lower frequency, movements of ions and polar moieties can follow the external electrical field as well. In polymeric materials, dipoles can be associated with side groups and/or the backbone. These dipoles may rotate according to the alternating electrical field. At low frequency or high temperature a certain class of dipoles can follow the applied electrical field. As the frictional force is low, the dielectric loss, which represents the absorbed energy, is low.

* Corresponding author: E-mail hsiaoyen_yang@hotmail.com

Received July 19, 2017; Accepted August 30, 2017; Published online January 15, 2018

At high frequency or low temperature, the friction force is high but the displacement is quite low. Thus the dielectric loss is low as well. For each specific relaxation process, the dielectric loss has a maximum at some specific combination of frequency and temperature. The inverse of the angular frequency at such a maximum corresponds to the characteristic time scale of a specific process at the given temperature.

Some studies on drawn semicrystalline polymers, such as poly(ethylene terephthalate)^[17], poly(ethylene naphthalene-2,6-dicarboxylate)^[18–20] and polyamide^[14, 21], show that cold drawing leads to a change of mobility in the amorphous part of the polymer. In the present investigation, DRS was used to study the effect of the draw ratio upon the molecular dynamics of PCL. There are three main relaxation processes in the measuring window, denoted α , β and γ in the order of increasing characteristic frequency (decreasing time scale) and decreasing temperature. The β and γ processes follow the Arrhenius law,

$$\ln \tau_{\beta,\gamma} = \ln \tau_{0,\beta,\gamma} + \frac{E_{\beta,\gamma}}{kT} \quad (1)$$

where $E_{\beta,\gamma}$ represents the activation energy of the β or γ relaxation processes, k is the Boltzmann constant, $\tau_{0,\beta,\gamma}$ is a prefactor, which is formally the limiting relaxation time of the β or γ process when $T \rightarrow \infty$. It is commonly found that the α process does not satisfy the Arrhenius law. It is often found useful to fit the data to the semi-empirical Vogel-Fulcher-Tammann (VFT) temperature dependency,

$$\ln \tau = \ln \tau_{0,\alpha} + \frac{A}{k(T - T_0)} \quad (2)$$

in which A is a parameter for a particular polymer, k is the Boltzmann constant, T_0 is the so-called Vogel temperature, at which the relaxation time diverges for a particular polymer, and $\tau_{0,\alpha}$ is formally the relaxation time of the α process when $T \rightarrow \infty$. The β and γ processes represent local relaxation modes, while the α process is a larger-scale cooperative motion. As it relates to the glass transition, it is often called the dynamic glass transition. The α process occurs in the amorphous part, while the β relaxation process may occur both in the amorphous and in the crystalline regions. The γ process represents even smaller-scale motions than the β process. Upon increasing temperature, the α and β relaxation time converge. Beyond the so-called crossover region, there are no longer separate α and β processes. Instead, there is a single relaxation that is often denoted the ‘ a process’ or ‘ $\alpha\beta$ process’^[22].

In the following sections, we will describe investigations on the effects of drawing upon the chain mobility of PCL by means of DRS and some complementary methods. We will discuss results on the dynamics in connection with observations on the morphology.

EXPERIMENTAL

Materials

Polycaprolactone (PCL) CAPA 6800 was kindly provided by Perstorp, U.K. and used as received. The molecular weight is

around 8×10^4 g/mol. Samples for drawing were prepared using a Davis Standard single screw extruder with a 19 mm screw and a length to diameter (L/D) ratio of 25, equipped with a melt pump in order to stabilize the melt pressure and ensure a constant flow out of the die. A flat tape die of 1 mm \times 16 mm was used. After leaving the die the material was cooled on adjustable chill rolls and thereafter drawn in the solid state at room temperature on a customized bench top drawing unit from Retech Switzerland. The temperature in the extruder was at its maximum 125 °C (at the die) and the temperature of the chill rolls was set to 21 °C. The speeds of the chill rolls and the first set of godet rolls in the drawing unit were set to match the melt pump speed so that no pre-orientation of the sample prior to drawing would occur. In order to obtain samples with different draw ratios, the speed of the second set of godets in the drawing equipment was varied. The resulting draw ratio equals the ratio between the speeds of the two sets of godet rolls, assuming that no slip occurs in the drawing process. The samples are named after their draw ratio. Undrawn samples were made as 9 mm wide and 0.5 mm thick strips. PCL is not elastically stretched but plastically drawn. When samples are elongated, necking occurs. Upon elongation of the sample, the draw ratio λ of the neck is 4 (the ‘natural draw ratio’). The fraction of the sample that turns into neck grows as the sample is more and more elongated. Samples with draw ratios > 4 are made by further stretching of the neck fraction.

Dielectric Relaxation Spectroscopy

Dielectric relaxation spectroscopy (DRS) was performed with a Novocontrol© Alpha High Resolution Analyzer broadband dielectric spectroscope. PCL samples with different draw ratios (namely $\lambda = 1$, $\lambda = 4$, $\lambda = 5$ and $\lambda = 8$) were measured in the frequency range $0.10905 \text{ Hz} \leq \omega/2\pi \leq 3 \text{ MHz}$, where ω is the angular frequency. All spectra were measured isothermally, at temperatures ranging from 20 °C to –120 °C, with a step of 2 °C. The cooling rate between each step is 10 K/min. The measuring temperatures were stabilized better than 0.5 °C using a PID circuit and a PT100 as temperature sensor. In order for the electrical field to be normal to the drawing direction, conventional copper electrodes were mounted onto the two sides of the sample. To obtain what we will call ‘apparent peak positions’, the dielectric loss permittivity was analysed in the temperature domain by spline-fitting. In addition, the dielectric loss permittivity was fitted by Cole-Cole peak shapes in the frequency domain. Several undrawn samples were measured in order to check reproducibility. The γ mode traces of different samples in the Arrhenius plot showed a relatively large variation, which may be caused by varying humidity and measurement error. The α mode trace also showed some variation between different undrawn samples. However, the shifts upon drawing were considerably larger than the variation between duplicate measurements.

Wide Angle X-ray Diffraction

Wide angle X-ray diffraction was performed with an AXS D8 Discover X-ray Diffractometer (Bruker-Nonius) to investigate the morphology and orientation of crystals in PCL samples with different draw ratios. The instrument was

equipped with cross-coupled Göbel mirrors to filter the Cu K α radiation ($\lambda = 0.154$ nm), and a Hi-Star 2D detector. The distance between sample and detector was 6 cm.

Differential Scanning Calorimetry

A Perkin Elmer Diamond DSC (Hyper DSC™) was used to perform differential scanning calorimetry (DSC) measurements. All samples were cooled down from 25 °C to -100 °C with a cooling rate of 10 K/min; then heated up to 100 °C with a heating rate of 10 K/min, and then cooled down again to 0 °C, with a cooling rate of 10 K/min.

RESULTS AND DISCUSSION

Results

3-D plots of the loss contribution of the dielectric permittivity versus frequency and temperature of undrawn and drawn PCL samples are shown in Fig. 1. There is a pronounced conduction peak in the dielectric loss at the high temperature,

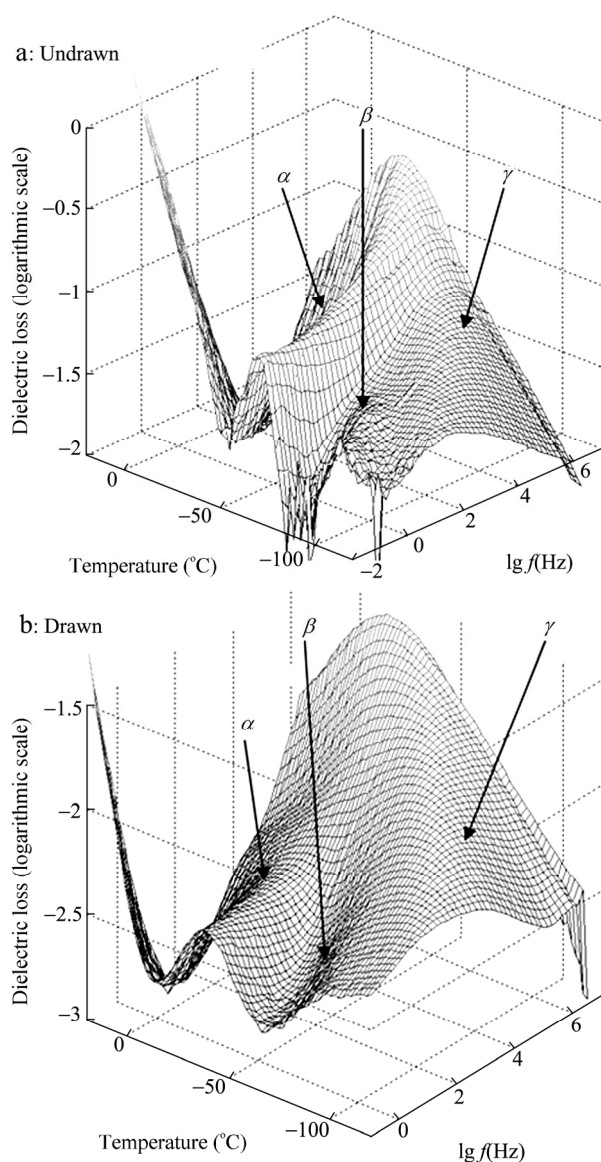


Fig. 1 3-D plot of dielectric loss versus frequency and temperature of PCL samples with (a) $\lambda = 1$, (b) $\lambda = 8$

low frequency regime, which overlaps with the relaxation peaks of interest. The undrawn sample (Fig. 1a) clearly shows three peaks, namely α , β and γ . The drawn samples (Fig. 1b) show an increase of the intensity of the γ peak as the draw ratio increases. This increase of the intensity of the γ peak leads to overlap with the β peak. As the β and γ peaks merge, it is difficult to analyse the relatively weak β peak. At a fixed frequency, the α relaxation shifts to higher temperature as the draw ratio increases. This is seen clearly in dielectric loss spectra in the temperature domain at different frequencies (Fig. 2). At low frequencies, e.g. 7.48 rad/s (Fig. 2a), the $\lambda =$

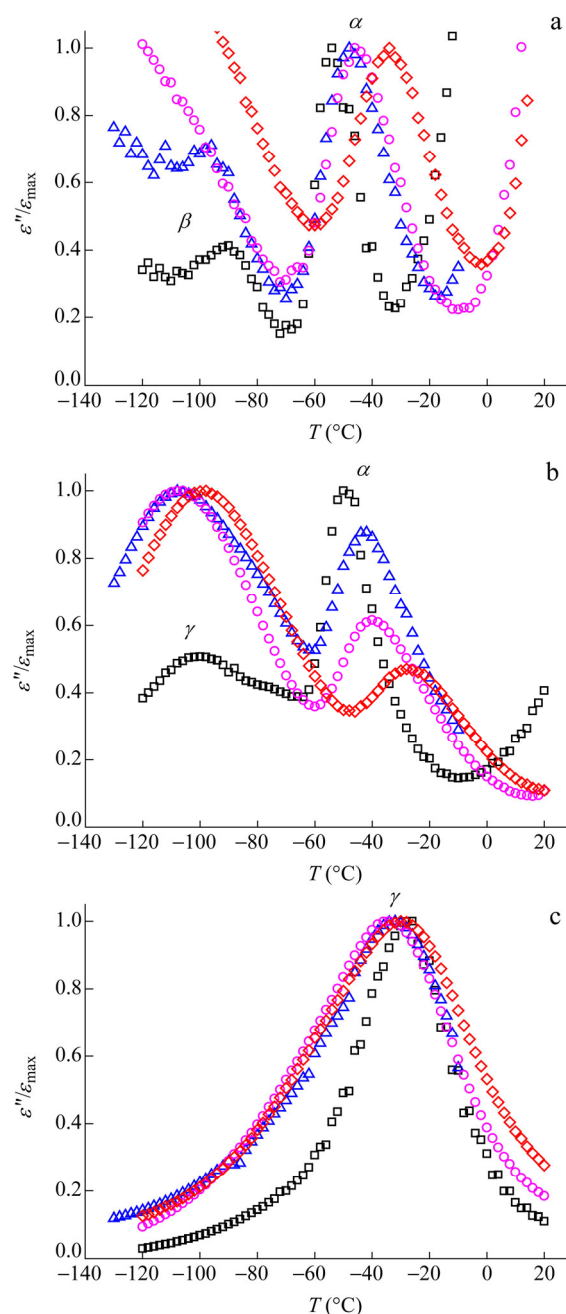


Fig. 2 Dielectric loss spectra of PCL with different draw ratios, $\lambda = 1$ (\square), $\lambda = 4$ (\triangle), $\lambda = 5$ (\circ), and $\lambda = 8$ (\diamond), in the temperature domain at different frequencies: (a) 7.48 rad/s, (b) 891 rad/s, (c) 8.5×10^6 rad/s

1 and $\lambda = 4$ samples show two peaks, at around -98 °C and -60 °C, representing the β and α relaxation processes, respectively. The low temperature peaks (β process) of the $\lambda = 5$ and $\lambda = 8$ samples are not clear. Therefore, for these low temperatures we cannot determine an accurate peak position for the β process to include in the Arrhenius plot (Fig. 3). The α process shifts to higher temperature as the draw ratio increases. As the frequency increases, for instance, to 8.91×10^2 rad/s (Fig. 2b), there are for all investigated draw ratios two peaks visible in the measured temperature range, which reflect the α and γ processes. The β peak is hidden under the γ peak. Both the α and γ peaks shift to higher temperature as the draw ratio increases, but the shift of the γ peak is quite small. In the high frequency range, at 8.5×10^6 rad/s for instance (Fig. 2c), for all measured samples there is only one peak visible in the measured temperature range, representing the γ process. The peak position shifts to higher temperature upon increasing frequency (Fig. 2).

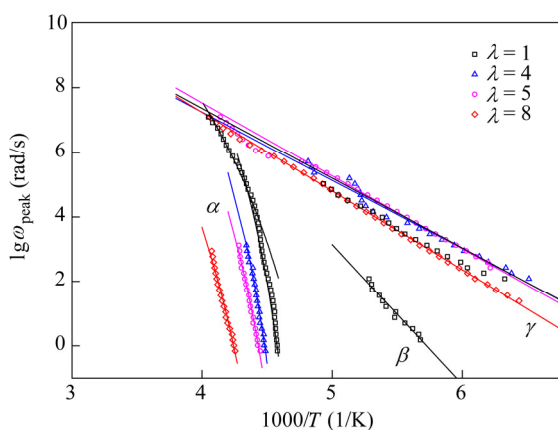


Fig. 3 Arrhenius plot of ‘apparent peak positions’ for PCL with different draw ratios, $\lambda = 1$ (\square), $\lambda = 4$ (\triangle), $\lambda = 5$ (\circ) and $\lambda = 8$ (\diamond) (Lines are for eye guiding. Points are obtained by spline-fitting the experimental dielectric loss in the temperature domain.)

Figure 3 is an Arrhenius plot of what we will denote the ‘apparent peak positions’. These are obtained by fitting spline functions to the dielectric loss spectra in the temperature domain. Points with the derivative value equal to zero and a negative second derivative are plotted in Fig. 3. Figure 3 clearly shows the α , β and γ relaxation processes for the undrawn sample. However, for the drawn samples the weak β peak merges with the strong γ peaks. Hence, no apparent β peak position can be determined and only the α and γ relaxation processes are plotted in Fig. 3. The α peak shifts to higher temperature/lower frequency as the draw ratio increases. For the γ mode trace, a relatively large variation was found between several independent measurements on undrawn samples. The reason for this may be the presence of traces of water, which may increase the intensity of the β peak^[23]. The enlarged β peak affects the apparent position of the γ peak. Anyway, this variation between measurements makes it impossible to reliably establish whether or not the γ peak position is really influenced by the draw ratio.

Spectra of the dielectric loss in the frequency domain of PCL samples with different draw ratios are shown in Fig. 4. At low temperature (e.g. -120 °C, as shown in Fig. 4d) the peak in the centre of the measured frequency window represents the γ process. The peak shifts to higher frequency as λ increases from 1 to 5. As the draw ratio increases further to 8, the peak position shifts back to lower frequency. Such shifts of the γ peak position upon drawing occur for all temperatures in the experimental range. At -90 °C, shown in Fig. 4(c), the β process appears in the measured frequency window. It is quite clear as a shoulder at about 10 Hz in the spectrum of undrawn sample. It is not so obvious in drawn samples. Comparing to Fig. 4(d), the γ peak positions shift to higher frequency upon increasing temperature. At -42 °C, shown in Fig. 4(b), shallow peaks appear at lower frequencies for the $\lambda = 4$ and $\lambda = 5$ samples. These represent the α process. With the undrawn sample, the α process occurs at higher frequency than that with $\lambda = 4$ and $\lambda = 5$, and it merges with the overlapping γ/β peak. Furthermore, for $\lambda = 8$, the α peak is still largely outside the measured frequency window. At -20 °C, shown in Fig. 4(a), it is quite clear that the α peak of the drawn samples appears in the measured frequency window. The α peak in the undrawn sample shifts to higher frequency and merges with the big γ/β peak as the temperature rises. The position of the α peak shifts to lower frequency upon increasing draw ratio.

As mentioned, all peaks in the loss spectra (partly) overlap, leading to shifts in apparent peak positions. Therefore, we have determined the true position and other characteristics of the overlapping peaks by fitting the experimental spectra with Cole-Cole (CC) peak shapes^[24]. The complete loss spectrum can be fitted to a series of CC peaks, and a conductivity term:

$$\varepsilon^* = \varepsilon_\infty + \sum_n \frac{\Delta\varepsilon}{1 + (i\omega\tau_n)^{a_n}} + \frac{i\sigma_0}{\varepsilon_0\omega} \quad (3)$$

$$\varepsilon' = \varepsilon_\infty + \sum_n \frac{\Delta\varepsilon(1 + \omega\tau_n)^{a_n} \cos\left(\frac{a_n\pi}{2}\right)}{1 + 2(\omega\tau_n)^{a_n} \cos\left(\frac{a_n\pi}{2}\right) + (\omega\tau_n)^{2a_n}} \quad (4)$$

$$\varepsilon'' = \frac{\sigma_0}{\varepsilon_0\omega} + \sum_n \frac{\Delta\varepsilon_n(\omega\tau_n)^{a_n} \sin\left(\frac{a_n\pi}{2}\right)}{1 + 2(\omega\tau_n)^{a_n} \cos\left(\frac{a_n\pi}{2}\right) + (\omega\tau_n)^{2a_n}} \quad (5)$$

where ε^* is the complex dielectric permittivity, ε' and ε'' are its real and imaginary part, respectively. The subscript n indicates a specific relaxation process, ω represents the angular frequency, ε_∞ is the permittivity at the high frequency limit ($\omega = \infty$), ε_0 is the dielectric permittivity at the low frequency limit ($\omega = 0$), $\Delta\varepsilon_n$ is the dielectric strength of relaxation process n , τ_n is the characteristic relaxation time for each process which is related to the frequency of maximal loss by $\tau_n = 1/\omega_{n,\text{peak}}$. a ($0 < a \leq 1$) is the shape parameter describing the width of a relaxation peak, which is determined by the width of the corresponding peak of the relaxation-time

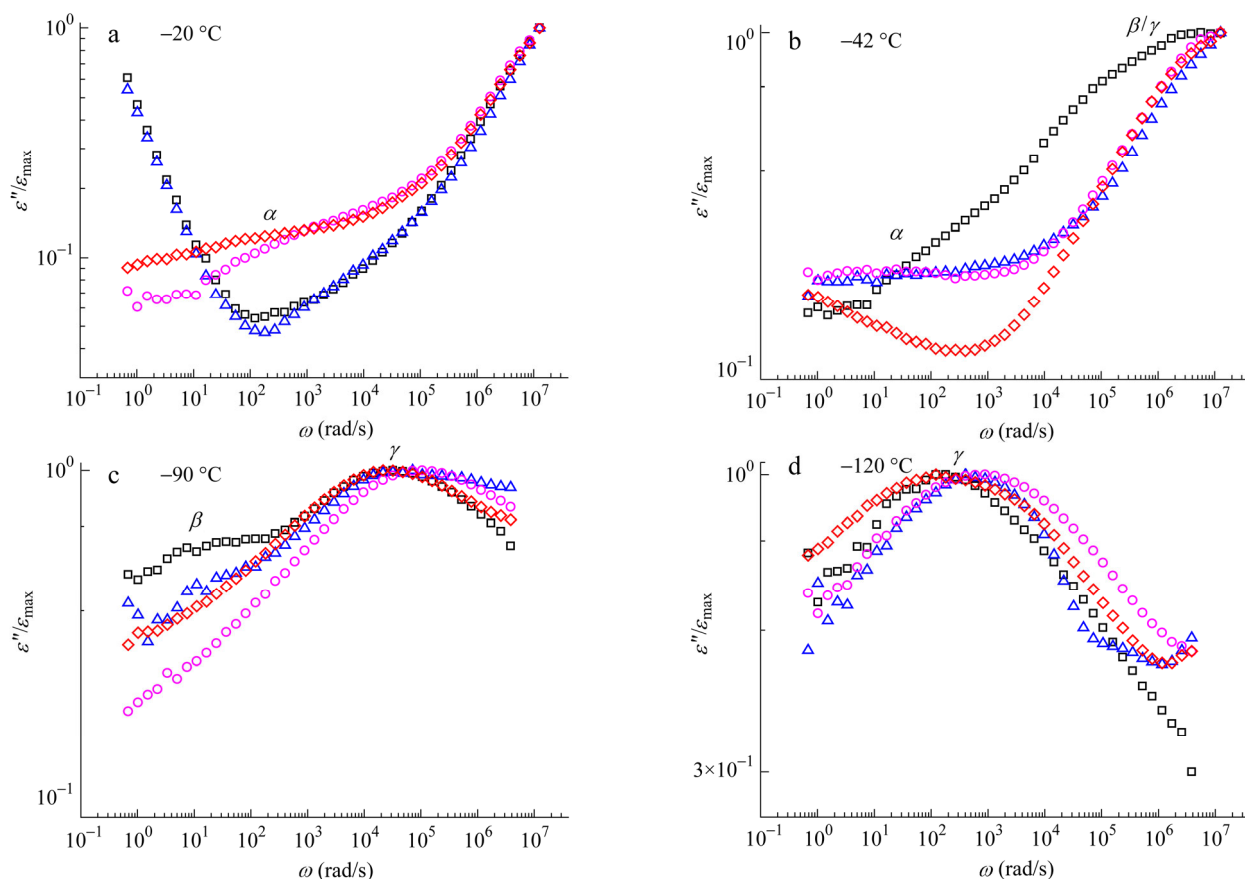


Fig. 4 Dielectric loss of PCL with different draw ratios, $\lambda = 1$ (\square), $\lambda = 4$ (\triangle), $\lambda = 5$ (\circ), and $\lambda = 8$ (\diamond), in the frequency domain at the different temperatures: (a) $-20\text{ }^{\circ}\text{C}$, (b) $-42\text{ }^{\circ}\text{C}$, (c) $-90\text{ }^{\circ}\text{C}$, and (d) $-120\text{ }^{\circ}\text{C}$

distribution. When $a = 1$, the CC equation reduces to the Debye equation, which represents a single-relaxation time process. σ_0 is related to the conductivity. Fitted parameters belonging to peaks near the edge of the measured frequency window have a somewhat larger uncertainty because of interference with relaxation peaks outside the measured frequency window.

The dielectric loss spectra have been interpreted with three processes, namely α , β , and γ , each represented by a Cole-Cole term. As known, the temperature dependence of the β and γ processes follows the Arrhenius law (Eq. 1). As described previously, the γ peak shifts to higher frequency as the temperature increases, and even shifts out of the measured frequency window above a certain temperature. However, the left wing of the peak then still contributes to the dielectric loss spectrum in the measuring range. So the fitting procedure started from the lowest measured temperature at which the dielectric loss spectrum shows clear β and/or γ relaxations. Based on the fitting parameters obtained at low temperatures, traces of the β and γ relaxation modes in the low temperature range in the Arrhenius plot can be obtained. According to the Arrhenius law, the positions of the β and γ peaks in the high temperature range can be obtained by extrapolation. For *e.g.* the undrawn sample, in the temperature range from $-120\text{ }^{\circ}\text{C}$ to $-50\text{ }^{\circ}\text{C}$, there are only β and γ peaks in the measured frequency window. As the temperature increases, the α process appears at around $-60\text{ }^{\circ}\text{C}$. From this temperature

upwards, there are three peaks within the measured frequency window, corresponding to the α , β , and γ relaxations. The characteristic frequencies are plotted against inverted temperature in Fig. 5. The α relaxation process shifts to higher temperature/lower frequency as the draw ratio increases.

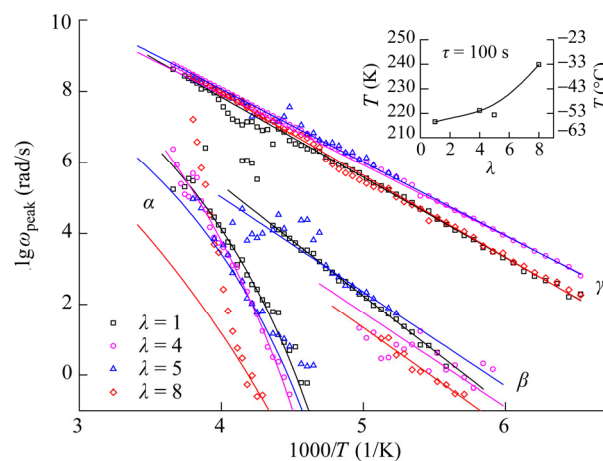


Fig. 5 Arrhenius plot of dielectric-loss peak positions for PCL with different draw ratios, as obtained by Cole-Cole fitting: $\lambda = 1$ (\square), $\lambda = 4$ (\triangle), $\lambda = 5$ (\circ) and $\lambda = 8$ (\diamond) (Straight lines follow the Arrhenius law. The α processes follows the VFT equation. The inset is the temperature at $\tau = 100$ s of samples of different draw ratio.)

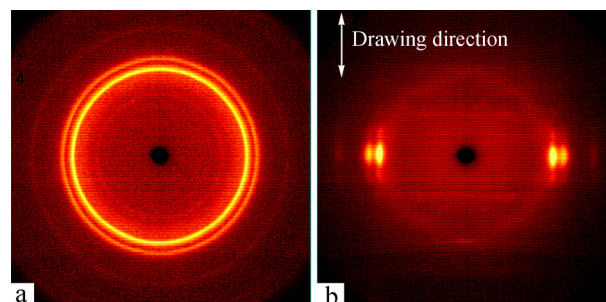
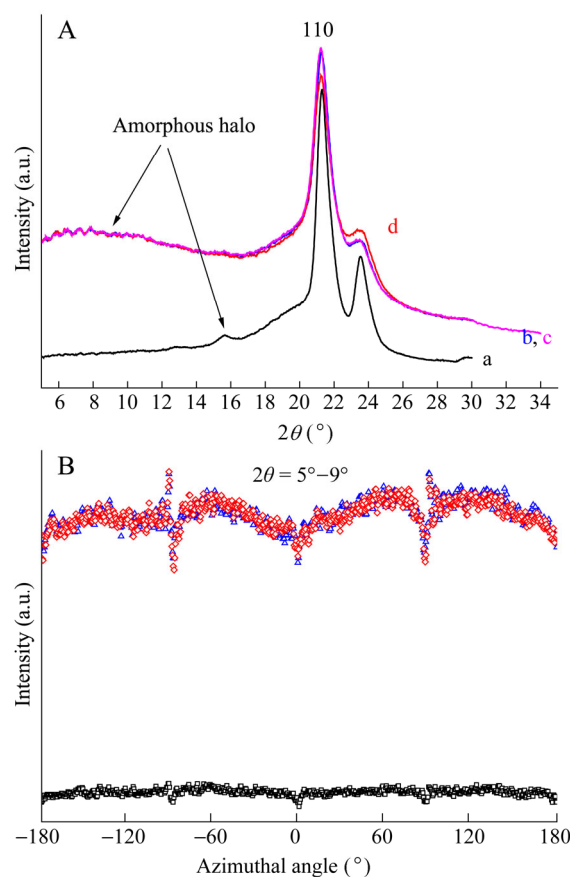
Table 1 The parameters of fitting different relaxation processes in Arrhenius plot (Fig. 5)

Relaxation process	γ		β		α		T_0 (K)	
	Draw ratio	$\tau_{0,\gamma}$ (s)	E_γ (eV)	$\tau_{0,\beta}$ (s)	E_β (eV)	$\tau_{0,\alpha}$ (s)		A (eV)
$\lambda = 1$		1×10^{-17}	0.45	1.5×10^{-18}	0.62	5.5×10^{-13}	0.16	160
$\lambda = 4$		1×10^{-16}	0.40	2×10^{-16}	0.53	8.9×10^{-14}	0.19	157.5
$\lambda = 5$		5×10^{-17}	0.41	8×10^{-16}	0.53	9.1×10^{-15}	0.21	155
$\lambda = 8$		7×10^{-18}	0.46	3×10^{-16}	0.5	6.6×10^{-14}	0.3	124

This trend is the same as found for the apparent peak positions plotted in Fig. 3. Furthermore, in the case of the α trace for the $\lambda = 8$ sample, there is a decrease (*i.e.* less negative) of the slope below about 1 rad/s. Even though the β relaxations appear hidden by the γ process in the spectra, the CC fitting procedure is capable of revealing its parameters. The slope in the Arrhenius plot of the β line for the drawn samples is slightly larger (less negative) as compared to that for the undrawn sample. This indicates a small decrease of the activation energy of the β relaxation process upon drawing. The γ trace in Fig. 5 is similar to that in Fig. 3. As described in the introduction section, the peak position corresponding to the α relaxation processes follows the VFT equation, and the β and γ relaxation modes follow the Arrhenius law. As for α relaxation process, a set of parameters were input initially, then the standard deviation between the experimental data and fitting data was minimized by modifying the pre-input parameters. At least five sets of initial parameters were input for each VFT fitting. For all investigated draw ratios the parameters of the VFT equation and the Arrhenius equations are listed in Table 1. The activation energies of the β and γ processes do not change significantly upon increasing draw ratio, while the VFT parameter A for the α process shows a significant increase upon drawing, especially for the highest drawing ratio. The Vogel temperature decreases upon increasing draw ratio.

Although the peak positions plotted in Figs. 3 and 5 were obtained from the dielectric spectra by very different methods, the shift of the α line upon drawing is clear with both methods. As the draw ratio increases, the α relaxation shifts to higher temperature/lower frequency. The glass transition is related to the α process, which is therefore called the dynamic glass transition. The glass-transition temperature is often defined somewhat arbitrarily as the temperature when the α relaxation time equals 100 s. The inset in Fig. 5 shows that the glass transition temperature according to this definition increases upon increasing draw ratio. Such an increase of the glass transition upon drawing was also found by others by means of a very different technique, namely dynamic mechanical thermal analysis (DMTA)^[25].

The X-ray diffraction results show that the crystals in undrawn PCL sample are randomly oriented (Fig. 6a), and that the crystals are oriented in drawn samples (Fig. 6b). The WAXS patterns of PCL with different draw ratios (Fig. 7A) show a clear amorphous halo at low 2θ range (5° – 9°) for the drawn samples. The intensity of the amorphous halo has been plotted as function of the azimuthal angle in Fig. 7(B). The features in the scattering signal at azimuthal angles -90° and 90° are caused by the wires holding the beam-stop in front of the detector. Compared to the undrawn sample, the drawn

**Fig. 6** Pictures of X-ray diffraction of PCL with draw ratios of (a) $\lambda = 1$ and (b) $\lambda = 8$ **Fig. 7** (A) WAXS patterns of PCL with draw ratios of (a) $\lambda = 1$, (b) $\lambda = 4$ (c) $\lambda = 5$ and (d) $\lambda = 8$; (B) WAXS intensity of the amorphous halo ($2\theta = 5^\circ$ – 9°) as a function of azimuthal angle for sample with draw ratios of $\lambda = 1$ (\square), $\lambda = 4$ (Δ), $\lambda = 5$ (\circ) and $\lambda = 8$ (\diamond) (The azimuthal angle of 90° is equatorial, and of 180° is meridional. The online version is colorful.)

samples show an increase of intensity of the amorphous halo. There are two broad peaks at azimuthal angles -90° and 90°

(Fig. 7B), indicating orientation along the drawing direction. As shown in Fig. 7(A), the widths of the amorphous halos of drawn samples are smaller than those of the undrawn sample.

The spectrum shown in Fig. 7(A) has been separated into several contributions, which are associated with crystallites and with the amorphous part. Our results indicate that drawing leads to alignment of crystals, but not to much change of the degree of crystallinity or the crystalline structure as such. DSC results (Fig. 8) confirm that the degree of crystallinity (which has been calculated based on the referenced data taken from Refs. [26] and [27]) is similar for different draw ratios. In this study, our main focus does not concern the crystal structure, but is aimed at the polymer chains in the amorphous part.

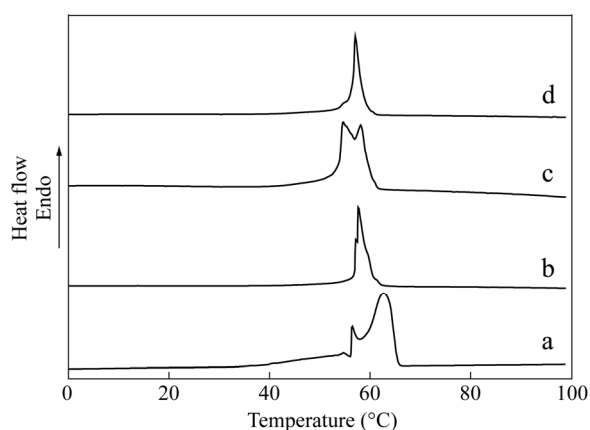


Fig. 8 Plot of DSC results of PCL with different draw ratios: (a) $\lambda = 1$, (b) $\lambda = 4$, (c) $\lambda = 5$ and (d) $\lambda = 8$, respectively (The heating rate is 10 K/min.)

Discussion

In Fig. 5, different relaxation mode traces for all investigated samples were fitted with the VFT equation (for the α relaxation) and the Arrhenius equations (for the β and γ relaxations). The parameters of the VFT and Arrhenius equations used in fitting are listed in Table 1. The parameters for the $\lambda = 1$ sample are similar to previously reported data for PCL, but not exactly the same^[23,28,29]. Comparing to those results, the difference can only be seen in the parameters for the β and γ relaxation modes. In Ref. [23], $E_\beta = (0.59 \pm 0.01)$ eV, $E_\gamma = (0.35 \pm 0.01)$ eV and $\tau_{0,\gamma} = 2 \times 10^{(-16 \pm 0.1)}$ s. In our results, E_β is 0.02 eV higher, E_γ is 0.07 eV higher, and the difference of $\tau_{0,\gamma}$ is $10^{\pm 0.8}$ s. The differences are most likely due to differences between the fitting approaches. The strategy used in Ref. [23] was to fit all the dielectric loss spectra with a set of parameters to achieve the global minimum of the difference between the fitting and experimental data. First, the spectra were fitted at temperatures where the different relaxation modes are best distinguished. The variation of the fitting parameters for successive temperatures was constrained to be smooth. However, to maintain such a smooth variation of the fitting parameters, the global minimum of the fitting may not always be reached. Our approach was to fit first the dielectric loss spectra in the low temperature range, in which only one or two relaxation modes (*i.e.* the β and/or γ processes) had to be

considered. Then the peak positions of β and/or γ processes in the high temperature range were extrapolated according to the Arrhenius equation.

The activation energies of local relaxation modes (*i.e.* β and γ relaxation processes) for the necking part ($\lambda = 4$) are slightly lower than those for the $\lambda = 1$ sample (Figs. 5 and 9). Upon further increase of the draw ratio, from $\lambda = 4$ to higher values, the activation energy of local relaxation modes increases somewhat. Lee *et al.*^[30] found that the segmental mobility in slightly cross-linked poly(methyl methacrylate) increases at low stress, then decreases at higher stresses. So our observation for PCL, that the activation energy of local relaxation modes decreases in the necking process (from $\lambda = 1$ to $\lambda = 4$) and then increases upon further drawing (from $\lambda = 4$ to $\lambda = 8$), is not unprecedented. Without further information we cannot give a molecular explanation for this observation. The β relaxation process occurs in both crystalline and amorphous regions^[31]. It represents local, small-scale dynamics, both in terms of size and time. In comparison to the β relaxation process, the γ process corresponds to an even smaller scale. Drawing does not significantly affect the β and γ relaxation processes. This is consistent with observations on drawn and undrawn low density polyethylene^[31].

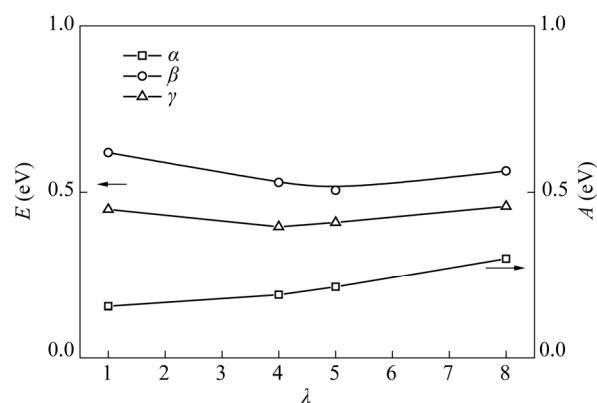


Fig. 9 Activation energy (Eq. 1) of the β (o) and γ (Δ) relaxation modes, and the parameter A (Eq. 2) of the α (\square) relaxation of samples with different draw ratios

The VFT equation (Eq. 2) was used to fit the α peak positions in the Arrhenius plot (Figs. 3 and 5). As the VFT equation is similar to the Arrhenius equation (Eq. 1), the parameter A in Eq. (2) is sometimes simply taken as the activation energy of the α process^[23,28]. This is not correct. Accepting this would *e.g.* imply that the activation energy of the α relaxation is smaller than that of the β and γ processes (Fig. 9). Obviously the activation energy for larger scale movements should be larger than that of smaller scale movement (β and γ processes). We introduce a temperature-dependent activation (free) energy E_α so that

$$\tau = \tau_0 e^{\frac{A}{k(T-T_0)}} = \tau_0 e^{\frac{E_\alpha}{kT}} \quad (6)$$

with activation (free) energy

$$E_{\alpha} = \frac{AT}{T - T_0} = A \left(1 - \frac{T_0}{T} \right)^{-1} \quad (T > T_0) \quad (7)$$

Thus, the activation energy of the α process according to the VFT equation, is a function of the temperature, and the Vogel temperature is the parameter that determines the temperature dependency. The larger the Vogel temperature, the stronger the activation energy increases upon decreasing temperature. This temperature dependency of the activation energy reflects the size increase of the ‘cooperatively rearranging region’ (CRR) associated with the α process.

As discussed extensively by Donth^[22], the a (or $\alpha\beta$) process corresponds to large-scale movements of chains escaping from cages of surrounding chains. As the temperature decreases, the increasing density enhances the trapping of chains by neighbours. Adam and Gibbs^[32] defined a cooperatively rearranging region (CRR) as a subsystem that can rearrange into another conformation upon a sufficient thermal fluctuation, independent of the environment. This concept has been further described, by Donth^[22], as the smallest functionally representative freely fluctuating subsystem of the α process. In the cage model^[22], the CRR can be interpreted as the cage wall thickness. Previous studies show that, in the crossover region, the a process does not connect with the α process but with the β process for poly(ethyl methacrylate)^[33] (scenario 1); however, the a process and the α process are continuous for bis-methoxy-phenyl-cyclohexane^[34] (scenario 2). Donth^[22] has proposed a molecular picture to interpret the two different scenarios in the crossover region. The difference is that scenario 2 corresponds to a larger cage wall thickness or a larger CRR than for scenario 1. A thicker cage wall makes both the a cage escape and the α cage escape more complex and difficult. The a cage is formed by dynamically nonequivalent molecules, while the α cage is built of dynamically equivalent molecules. In scenario 1, approaching the crossover region from high temperature, the α process and the a process exist simultaneously, but escape from the α cage is slower than from the a cage. In scenario 2, as temperature decreases, the a process and the α process need a larger ‘door’ and diffusion over larger distances is needed to escape from the cage. Thus, escape from a cage requires a larger number of attempts to succeed. Therefore, near the crossover region, the a process and the α process are similar, while the difference between the a process and the β process is larger than for scenario 1. This results in the continuity of the a process and the α process, and the separation of the a process and the β process traces.

Drawing affects the α process as it corresponds to the cooperative motion of the local environment^[31, 35]. Such cooperative motions are influenced by structural changes, such as the above-mentioned straining, aligning and densification caused by drawing. In terms of free volume theory, the latter implies a decrease of free volume. These structural changes lead to an increase of the size of the ‘cooperatively rearranging region’ (CRR) associated with the α process. In terms of the cage model, this means that the ‘cage wall thickness’ increases. As the draw ratio increases,

the α relaxation broadens and the intensity decreases (Fig. 2). The broadened peak indicates a broader relaxation-time distribution. The area of the α peak reflects the amount and magnitude of the dipoles responding to the applied alternating electrical field. Therefore, given that the total amount of dipoles does not change, the broader the relaxation time distribution, the lower the intensity of the peak.

Interestingly, we observe in Fig. 5 a change of the features of the cross-over region upon drawing. For the undrawn sample, we see that the a process does not connect with the extrapolation of the α process, and that the a process is continuous with the β process (scenario 1, as discussed above). Upon drawing we see that the crossover changes to a ‘scenario 2 type’, for which the a process is continuous with the α process. For the $\lambda = 8$ sample, the a process clearly connects in a continuous way with the α process as temperature decreases. These two different scenarios in the crossover region have been found in different polymers^[33, 34]. But, according to the authors’ knowledge, a change upon drawing from one scenario to the other in one polymer system has not been found before. When we interpret this change of the appearance of the cross-over region in the Arrhenius plot in terms of the molecular model proposed by Donth^[22] (as briefly reviewed in the introduction section), this implies an increase upon drawing of the size of the ‘cooperatively rearranging region’ (CRR) of the a and α processes. Stated slightly differently, this implies an increase of the thickness of the cage wall upon drawing. Apparently, drawing leads to an increased hindering between molecules (an increased cage effect), and a slowdown of the cooperative a and α processes^[36]. Thus, we interpret our experimental results as follows: when the necking part is stretched further to large ratios, e.g. $\lambda = 5$ and $\lambda = 8$, the polymer chains in the amorphous part are further stretched in the drawing direction and compressed in the transverse direction. The more compact ordering of polymer chains in the amorphous region lowers the free volume in the drawn samples. This leads to a thickening of the cage wall, or in other words, to an increase of the CRR size corresponding to the α process. Consequently, the apparent activation energy, which is related to the slope of the α trace in the Arrhenius plot, increases as the draw ratio increases. Furthermore, because the CRR size increases, it becomes more difficult to escape from the cage. Thus, the relaxation time of the cooperative movement of polymer chains (α relaxation) at a certain temperature increases as the draw ratio increases (Fig. 5). This is consistent with observations of other semicrystalline polymers, such as drawn low-density polyethylene^[31] and drawn polyethylene terephthalate^[37].

In undrawn PCL ($\lambda = 1$), the amorphous regions are isotropic and the crystallites are oriented randomly. When the sample is stretched, necking occurs, resulting in a drawn material with a natural draw ratio, $\lambda = 4$. Drawing orients crystals along the drawing direction (Fig. 6) accompanied by a conversion of spherulites to oriented fibrils^[8, 15, 38] and a possible recrystallization under strain^[16]. The polymer chains in the amorphous phase are constrained by entanglements and crystals. In the amorphous part of a $\lambda = 1$ sample, the

conformation distribution of the polymer chains is considered to be relaxed. Upon drawing, the polymer chains are stretched and oriented, as the distances between the entanglements and crystals increase along the drawing direction. The change from isotropic to anisotropic is confirmed by X-ray results (Fig. 6). According to Murthy *et al.*^[39], X-ray scattering with Cu K α radiation in the angular range $5^\circ \leq 2\theta \leq 35^\circ$ is mainly interchain scattering. Moreover, they demonstrated that ‘changes in amorphous density were reflected in the changes in the widths and positions of the amorphous halo’. Accordingly, they showed for polystyrene, polyethylene and nylon 6 that drawing orients the polymer chains in the amorphous part, and leads to denser packing. We observe in PCL a similar decrease of the width of the amorphous halo upon drawing (Fig. 7). This indicates similar structural changes upon drawing (*e.g.* chain orientation and a denser packing) in PCL.

As shown in Fig. 5, when the temperature decreases below that at which $\omega\alpha \approx 1$ rad/s, the slope of the α trace of the $\lambda = 8$ sample decreases (becomes less negative). This may be caused by the following reasons. (1) During cooling, the internal dynamics of the system (the α process) increasingly slow down, until at a certain temperature the internal dynamics are too slow to allow the system to adapt to further cooling. This is the glass transition. When cooled further, the system is no longer at equilibrium. This departure from equilibrium is accompanied by a change of the further temperature dependency of several physical properties, *e.g.* the temperature dependency of the volume. Similarly, a change of the temperature dependency of the α relaxation time itself would be expected^[40]. (2) Previous DRS measurements of polymers in zeolitic and nanoporous media^[41, 42] show a similar change of the temperature dependency of the α trace in the Arrhenius plot. A slope change like this has also been found to be caused by geometric confinement of polymer chains^[22, 41]. The perturbation of the conformation distribution of polymer chains upon drawing is similar to that under geometric confinement. Thus, the conformation change of polymer chains in the amorphous part upon drawing may cause the slope change of the α mode trace.

CONCLUSIONS

Drawing orients the crystals and the polymer chains in the amorphous part, but does not lead to a significant change of the degree of crystallization or the crystal structure. The stretching and ordering of polymer chains in the amorphous part result in a relatively compact structure and a decrease of the free volume. This leads to a change of the activation energy of relaxation processes. The α relaxation shifts to higher temperature/lower frequency, which yields an increase of the glass-transition temperature, and the relaxation time distribution of the α process broadens. This can be interpreted in terms of changes the CRR size. These changes result subsequently in a change of the continuity in the crossover between the high-temperature a process and the α and β processes.

ACKNOWLEDGMENTS

This research forms part of the research programme of the Dutch Polymer Institute (DPI), project#623.

REFERENCES

- Omid, Y.; Hamid, G. Development of a simple model to characterize the complex constrained polymer chains in polymer nanocomposites at the interphase of amorphous/semicrystalline ethylene vinyl acetate and nanosheets. *J. Compos. Mater.* 2016, 51(2), 179–186.
- Perez-de-Eulate, N. G.; Di Lisio, V.; Cangialosi, D. Glass Transition and Molecular Dynamics in Polystyrene Nanospheres by Fast Scanning Calorimetry. *ACS Macro Lett.* 2017, 6(6), 859–863.
- Sharma, R. P.; Green, P. F. Role of “Hard” and “soft” confinement on polymer dynamics at the nanoscale. *ACS Macro Lett.* 2017, 6(9), 908–914.
- Lee, K. H.; Kim, H. Y.; Khil, M. S.; Ra, Y. M.; Lee, D. R. Characterization of nano-structured poly(ϵ -caprolactone) nonwoven mats *via* electrospinning. *Polymer.* 2003, 44(4), 1287–1294.
- Chen, Z.; Cao, L.; Wang, L.; Zhu, H.; Jiang, H. Effect of fiber structure on the properties of the electrospun hybrid membranes composed of poly(ϵ -caprolactone) and gelatin. *J. Appl. Polym. Sci.* 2013, 127(6), 4225–4232.
- Bernards, D. A.; Bhisitkul, R. B.; Wynn, P.; Steedman, M. R.; Lee, O. T.; Wong, F.; Thoongsuwan, S.; Desai, T. A. Ocular Biocompatibility and Structural Integrity of Micro- and Nanostructured Poly(caprolactone) Films. *J. Ocul. Pharmacol. Th.* 2013, 29(2), 249–257.
- Shan, G. F.; Yang, W.; Yang, M. B.; Xie, B. H.; Fu, Q.; Mai, Y. W. Investigation on tensile deformation behavior of semi-crystalline polymers. *J. Macromol. Sci. B* 2009, 48(7), 799–811.
- Li, H.; Zhou, W.; Ji, Y.; Hong, Z.; Miao, B.; Li, X.; Zhang, J.; Qi, Z.; Wang, X.; Li, L.; Li, Z. M. Spatial distribution of crystal orientation in neck propagation: An *in-situ* microscopic infrared imaging study on polyethylene. *Polymer* 2013, 54(2), 972–979.
- Li, J. X.; Cheung, W. L.; Chan, C. M. On deformation mechanisms of β -polypropylene 3. Lamella structures after necking and cold drawing. *Polymer* 1999, 40(13), 3641–3656.
- Peterlin, A.; Molecular model of drawing polyethylene and polypropylene. *J. Mater. Sci.* 1971, 6(6), 490–508.
- Van Aerle, N. A. J. M.; Braam, A. W. M. A structural study on solid state drawing of solution-crystallized ultra-high molecular weight polyethylene. *J. Mater. Sci.* 1988, 23(12), 4429–4436.
- Mcrae, M. A.; Maddams, W. F.; Preedy, J. E. An infra-red spectroscopic and X-ray diffraction study of cold-drawn high density polyethylene samples. *J. Mater. Sci.* 1976, 11(11), 2036–2044.
- Flory, P. J.; Yoon, D. Y. Molecular morphology in semicrystalline polymers. *Nature* 1978, 272(5650), 226–229.
- Nozue, Y.; Shinohara, Y.; Ogawa, Y.; Takamizawa, T.; Sakurai, T.; Kasahara, T.; Yamaguchi, N.; Yagi, N.; Amemiya, Y. Deformation behavior of banded spherulite during drawing investigated by simultaneous microbeam SAXS-WAXS and POM measurement. *Polymer* 2010, 51(1), 222–231.
- Li, J. X.; Cheung, W. L. On the deformation mechanisms of β -polypropylene: 1. Effect of necking on β -phase PP crystals. *Polymer* 1998, 39(26), 6935–6940.
- Zhao, Y.; Keroack, D.; Prud'homme, R. Crystallization under strain and resultant orientation of poly(ϵ -caprolactone) in

- miscible blends. *Macromolecules* 1999, 32(4), 1218–1225.
- 17 Pieruccini, M.; Ezquerra, T. A.; Lanza, M. Phenomenological model for the confined dynamics in semicrystalline polymers: the multiple α relaxation in cold-crystallized poly(ethylene terephthalate). *J. Chem. Phys.* 2007, 127(10), DOI: 10.1063/1.2771166
- 18 Hakme, C.; Stevenson, I.; David, L.; Sixou, B.; Voice, A.; Seytre, G.; Boiteux, G. Molecular mobility in poly(ethylene naphthalene 2,6 dicarboxylate) (PEN) dielectric films. *Proceeding of the 2004 IEEE International Conference on Solid Dielectrics*. 2004, Vol. 1, 37–40.
- 19 Hakme, C.; Stevenson, I.; David, L.; Seytre, G.; Boiteux, G. Effect of orientation and crystallization on dielectric and mechanical relaxations in uniaxially stretched poly(ethylene naphthalene 2,6 dicarboxylate) (PEN) films. *J. Non-Cryst. Solids* 2006, 352(42-49), 4746–4752.
- 20 Nogales, A.; Denchev, Z.; Šics, I.; Ezquerra, T. A. Influence of the crystalline structure in the segmental mobility of semicrystalline polymers: poly(ethylene naphthalene-2,6-dicarboxylate). *Macromolecules* 2000, 33(25), 9367–9375.
- 21 Frübing, P.; Kremmer, A.; Gerhard-Multhaupt, R.; Spanoudaki, A.; Pissis, P. Relaxation processes at the glass transition in polyamide 11: from rigidity to viscoelasticity. *J. Chem. Phys.* 2006, 125(21), DOI: 10.1063/1.2360266
- 22 Donth, E. *The glass transition: relaxation dynamics in liquids and disordered materials*, Springer-Verlag Berlin Heidelberg, New York, 2001, p. 199.
- 23 Grimau, M.; Laredo, E.; Pérez, Y. M.; Bello, C. A. Study of dielectric relaxation modes in poly(ϵ -caprolactone): molecular weight, water sorption, and merging effects. *J. Chem. Phys.* 2001, 114(15), 6417–6425.
- 24 Scönhals, A.; Kremer, F., in “Broadband dielectric spectroscopy” ed. by Kremer, F.; Scönhals, A., Springer-Verlag Berlin Heidelberg, New York, 2003, p. 59.
- 25 Alcock, B.; Cabrera, N. O.; Barkoula, N. M.; Reynolds, C. T.; Govaert, L. E.; Peijs, T. The effect of temperature and strain rate on the mechanical properties of highly oriented polypropylene tapes and all-polypropylene composites. *Compos. Sci. Technol.* 2007, 67(10), 2061–2070.
- 26 Qiu, Z.; Yang, W.; Ikehara, T.; Nishi, T. Miscibility and crystallization behavior of biodegradable blends of two aliphatic polyesters. Poly(3-hydroxybutyrate-co-hydroxyvalerate) and poly(ϵ -caprolactone). *Polymer* 2005, 46(25), 11814–11819.
- 27 Crescenzi, V.; Manzini, G.; Calzolari, G.; Borri, C. Thermodynamics of fusion of poly- β -propiolactone and poly- ϵ -caprolactone. comparative analysis of the melting of aliphatic polylactone and polyester chains. *Eur. Polym. J.* 1972, 8(3), 449–463.
- 28 Bello, A.; Laredo, E.; Grimau, M. Comparison of analysis of dielectric spectra of PCL in the ϵ^* and the M^* formalism. *J. Non-Cryst. Solids*. 2007, 353(47-51), 4283–4287.
- 29 Serra, R. S. I. J.; Ivirico, L. E.; Dueñas, J. M. M.; Balado, A. A.; Ribelles, J. L. G.; Sánchez, M. S. Segmental dynamics in poly(ϵ -caprolactone)/poly(L-lactide) copolymer networks. *J. Polym. Sci., Part B: Polym. Phys.* 2009, 47(2), 183–193.
- 30 Lee, H.; Paeng, K.; Swallen, S. F.; Ediger, M. D. Direct measurement of molecular mobility in actively deformed polymer glasses. *Science* 2009, 323(5911), 231–234.
- 31 Suljovrujić, E. Dielectric studies of molecular β -relaxation in low density polyethylene: the influence of drawing and ionizing radiation. *Polymer* 2002, 43(22), 5969–5978. (Note: the β and γ relaxations in the reference are the α and β relaxations in this paper, respectively)
- 32 Adam, G.; Gibbs, J. H. On the temperature dependence of cooperative relaxation properties in glass-forming liquids. *J. Chem. Phys.* 1965, 143(1), 139–146.
- 33 Schröter, K.; Unger, R.; Reissig, S.; Garwe, F.; Kahle, S.; Beiner, M.; Donth, E. Dielectric spectroscopy in the $\alpha\beta$ splitting region of glass transition in poly(ethyl methacrylate) and poly(*n*-butyl methacrylate): different evaluation methods and experimental conditions. *Macromolecules* 1998, 31(25), 8966–8972.
- 34 Hansen, C.; Stickel, F.; Berger, T.; Richert, R.; Fischer, E. W. Dynamics of glass-forming liquids. III. Comparing the dielectric α - and β -relaxation of 1-propanol and *o*-terphenyl. *J. Chem. Phys.* 1997, 107(4), 1086–1093.
- 35 Smith, G. D.; Bedrov, D. Relationship between the α - and β -relaxation processes in amorphous polymers: Insight from atomistic molecular dynamics simulations of 1,4-polybutadiene melts and blends. *J. Polym. Sci., Part B: Polym. Phys.* 2007, 45(6), 627–643.
- 36 Götze, W. in “Liquid, Freezing and the Glass Transition”, ed. by Hansen, J. P.; Levesque, D.; Zinn-Justin, J., North-Holland, Amsterdam, 1991, p. 287.
- 37 Saiter, J. M.; Grenet, J.; Saiter, E. A.; Delbreilh, L. Glass Transition temperature and value of the relaxation time at T_g in vitreous polymers. *Macromol. Symp.* 2007, 258(1), 152–161.
- 38 Li, J. X.; Cheung, W. L.; Chan, C. M. On deformation mechanisms of β -polypropylene 2. changes of lamellar structure caused by tensile load. *Polymer* 1999, 40(8), 2089–2102.
- 39 Murthy, N. S.; Minor, H.; Bednarczyk, C. Structure of the amorphous phase in oriented polymers. *Macromolecules* 1993, 26(7), 1712–1721.
- 40 Liedermann, K. A simple formula for the temperature dependence of the relaxation frequency in glassy systems. *Collid. Polym. Sci.* 1996, 274(1), 20–26.
- 41 Kremer F.; Huwe A.; Scönhals A.; Rózański S. A., in “Broadband dielectric spectroscopy” ed. by Kremer, F.; Scönhals, A., Springer-Verlag Berlin Heidelberg, New York, 2003, p. 171.
- 42 Arndt, M.; Stannarius, R.; Groothues, H.; Hempel, E.; Kremer, F. Length Scale of Cooperativity in the Dynamic Glass Transition. *Phys. Rev. Lett.* 1997, 79(11), 2077–2080.